Polyhedron 67 (2014) 471–480

Contents lists available at ScienceDirect

Polyhedron

journal homepage: www.elsevier.com/locate/poly

Photoinduced linkage isomerization in new rhenium(I) tricarbonyl complexes coordinated to N-nitrite and O-nitrite

Sofía E. Domínguez [a], Pablo Alborés [b], Florencia Fagalde [a,*]

[a] INQUINOA-CONICET, Instituto de Química Física, Facultad de Bioquímica, Química y Farmacia, Universidad Nacional de Tucumán, Ayacucho 471, (T4000INI) San Miguel de Tucumán, Argentina
[b] Departamento de Química Inorgánica, Analítica y Química Física, INQUIMAE, Facultad de Ciencias Exactas y Naturales, Universidad de Buenos Aires, Pabellón 2, Ciudad Universitaria, C1428EHA Buenos Aires, Argentina

ARTICLE INFO

Article history:
Received 7 May 2013
Accepted 7 October 2013
Available online 10 October 2013

Keywords:
Nitro
Nitrito
Rhenium(I) tricarbonyl
Photoinduced linkage isomerization

ABSTRACT

The ambidentate nitrite ion, NO_2^-, is a biologically relevant species that can be coordinated to transition metals via the nitrogen or oxygen atom. Most of its physiological effects involve metalloproteins so it is important to understand the factors that control the predominance of one or another isomer. In this work, we present the syntheses and characterization by spectroscopy, electrochemistry and DFT calculations of new rhenium(I) tricarbonyl complexes with different polypyridyl ligands in the coordination sphere and with the nitrite ion coordinated through either its N- or O-atom. For two of them we have determined their crystal structures by X-ray diffraction and we have found that in the solid when the ancilliary ligand is bpy the N-binding mode is the most stable, while dmb is the ligand, the $-CH_3$ substituents imposed the C–H (methyl group)···O–NO (nitrito) interactions favoring the O-binding mode. However, at room temperature in CH_2Cl_2 the nitro isomer is the most stable for both complexes in agreement with DFT calculations. Both complexes exhibit photoinduced linkage isomerism which could be of interesting in the design of new materials. Although nitro complexes are precursors of nitrosyl compounds, in this work the synthesis of the nitrosyl complexes as solid could not be possible because there is higher π-backbonding from Re(I) to the carbonyl groups, or to the polypyridil ligands instead of to the NO group, which is π-acceptor, in consequence the nitrosyl complexes are unstable and decompose immediately to the solvate complexes.

1. Introduction

It is well known that nitrite ion, NO_2^-, is an ambidentate ligand which can coordinate through either the O- or N-atom, generating linkage isomerism in nitrite species. When the ion NO_2^- is coordinated via the nitrogen atom, the resulting M–NO_2 species is termed as "N- nitrite or nitro" complex, while when is coordinated via an oxygen atom, the M-ONO species is termed as "O-nitrite or nitrito" complex. The first example of linkage isomerism extensively studies was the fast isomerization of pentaamminenitritecobalt(III) ion bounded through either O- or N-, discovered by Jörgensen in 1894 and extensively studied by Alfred Werner (Nobel Prize in Chemistry in 1913) [1], where the O-nitrite complexes isomerizes spontaneously and stereo-retentively to the more stable N-nitrite complex. Kinetics and thermodynamic of NO_2/ONO interconversion investigated by thermal methods shows that N-nitro isomer is more stable than O-nitrite and isomerism could occur simultaneously both in solution and solid state [2].

In contrast with Co(III), Cr(III) binds nitrite ions as the nitrito isomers [3]. Generally, the relative stability of linkage isomers is associated with the sigma-donating tendencies of the two donor atoms of the ambidentate ligand: the stronger is the donor atom, the stable is the isomer. Moreover, steric effects play a decisive role, when both binding modes involve different steric hindrances toward co-ligands present in the coordination sphere. For instance, it is interesting to note that the pyridine rings in $Ni(py)_4(ONO)_2$ provide sufficient repulsion to cause the formation of a stable nitrito rather than a nitro complex [4].

On the other hand, complexes of transition metals, in particular Ru(II)/(III) and Os(II)/(III), with nitrite ion have been studied due to the interesting reactivity of the coordinated nitro ligand, with emphasis in the potential use of these complexes as nitro based oxygen atom transfer catalysts and because to their use as synthetic precursors for nitrosyl complexes [5]. Most of the mechanisms proposed for these reactions involves linkage isomerization of the coordinated nitrite ion [6–9]. In addition, photoinduced conversion between isomers in complexes with nitrite at the solid state, could be interesting in the design of new material with

* Corresponding author. Tel.: +54 3814247752; fax: +54 3814248169.
E-mail addresses: sedominguez@fbqf.unt.edu.ar (S.E. Domínguez), albores@qi.fcen.uba.ar (P. Alborés), ffagalde@fbqf.unt.edu.ar (F. Fagalde).
URL: http://www.inquinoa.org.ar (F. Fagalde).

0277-5387/$ - see front matter © 2013 Elsevier Ltd. All rights reserved.
http://dx.doi.org/10.1016/j.poly.2013.10.002

technological applies [10]. Related with the biological properties of the nitrite ion, Meyer and co-workers [11,12] described in detail the reduction of nitrite to ammonia using nitro complexes of Ru and Os, in order to model the reaction catalyzed by enzymes in the redox cycle of nitrogen .

For a long time, the nitrite ion was considered a dead end product of the metabolism of nitric oxide, until recently that it has received more attention due to the discovery of its physiological properties. This anion is the major vascular storage of NO [2a], and its roles in mammalian physiology includes hypoxic vasodilatation [13,14], cytoprotection in ischemia/reperfusion injury [15] and its potential use as therapeutic drug in the treatment of these diseases, [16] signaling [17] and regulation of gene expression in tissues.[18] Additionally, it was found that in ferriheme models and proteins the reductive nitrosylation is strongly catalyzed by nitrite ion [19,20], a product of this reaction, illustrating the importance of other NO_x species, and not only NO, in biological processes [21,22].

For proteins and heme models coordinated to nitrite [23] the N-binding mode is the most common; however, recently two crystal structures of heme proteins (one of them human hemoglobin) with nitrite coordinated via the O-binding mode have been reported [24,25]. Besides, it has been found that H-bonding with pocket residues directs the occurrence of that isomer [26]. The differences of energy between isomers have been calculated as relatively small, and reaction mechanisms involving both isomers are viable and correlate well with experimental data for these reactions [27,28]. Thus the chemical reactivity of nitrite ion is a function of the binding modes, and understanding the types of binding modes and the factors that determine them is important to unravel the chemical properties of this metabolite [29].

In this work, we present for the first time, the synthesis and characterization by spectroscopy and electrochemistry of new rhenium(I) tricarbonyl complexes with different polypyridyl ligands in the coordination sphere and with the nitrite ion in the N- and O-binding mode: [Re(bpy)(CO)$_3$(NO$_2$)] (**1**), [Re(bpy)(CO)$_3$(ONO)] (**2**), [Re(dmb)(CO)$_3$(NO$_2$)] (**3**) and [Re(dmb)(CO)$_3$(ONO)] (**4**), where bpy = 2,2′-bipyridine and dmb = 4,4′-dimethyl-2,2′-bipyridine. The experimental studies have been accompanied by elemental analysis and DFT and TDDFT calculations. For complexes (**1**) and (**4**) the structures have been confirmed by X-ray diffraction. Global chemical reactivity descriptors such as chemical hadness (η), electrophilicity (ω), and electronic chemical potentials (μ) [30] are calculated and used to probe the relative stability and reactivity of compounds (**1**) to (**4**). Although nitro complexes are precursors of nitrosyl compounds, in this work the synthesis as solid of the nitrosyl complexes derived from (**1**) and (**3**) could not be possible because there is higher π-backbonding from Re(I) to the carbonyl groups, bpy or dmb instead of to the NO group, which is π- acceptor, in consequence the nitrosyl complexes are unstable and decompose immediately to the solvate complexes. Though, work in progress will be done, to confirm that nitrosyl complexes could be form in solution by oxidation at higher potential of the nitro complexes.

2. Experimental

2.1. Materials and instrumentation

All chemicals used were analytical reagent grade. CH_2Cl_2 (anhydrous from Sigma–Aldrich) and CH_3CN (freshly distilled over P_4O_{10}) were used for electrochemical and luminescence measurements. UV–Vis absorption spectra were recorded on a Varian Cary 50 spectrophotometer, using 1-cm quartz cells. Infrared spectra were obtained with a Perkin-Elmer Spectrum RX-1 FTIR spectrometer as KBr pellets for solid samples and in a demountable sealed cell from Perkin-Elmer with AgCl windows for solutions. Cyclic voltammetry experiments were carried out using a BAS Epsilon EC equipment, with vitreous C as working electrode, Pt wire as auxiliary electrode, and Ag/AgCl (3 M NaCl) as reference electrode. Solutions were prepared in CH_2Cl_2 anhydrous or CH_3CN distilled and dried over molecular sieves with 0.1 M $TBAPF_6$ (*tetra*-n-butylammonium hexafluorophosphate) dried at 150° for 24 h as supporting electrolyte, protected of light and degassed for 15 min with Ar prior to each measurement. Controlled potential electrolyses were performed using an SEC-C thin layer quartz glass spectroelectrochemical cell from ALS, with Pt gauze as working electrode, Pt wire as counter electrode and Ag/AgCl (3 M NaCl) as reference electrode. Emission spectra were measured with a Shimadzu RF-5301 PC spectrofluorometer, provided with 1-cm fluorescence cells; solutions were protected of light and deoxygenated with Ar prior to measurements. Emission quantum yields were calculated in CH_2Cl_2 using Eq. (1), where: 1, 2 are referred to complex and reference respectively, Φ_2 quantum yield of $[Ru(bpy)_3]^{2+}$, n refractive index of solvent, A peak area and I intensity of absorption at wavelength of the MLCT. Chemical analyses for C, H and N were carried out at INQUIMAE, University of Buenos Aires, Argentina, with an estimated error of ±0.5%. Mass Spectra (ESI) was recorded at UMYMFOR, University of Buenos Aires, Argentina.

$$\phi_1 = \phi_2 \left(\frac{l_2}{l_1}\right)\left(\frac{n_2}{n_1}\right)^2\left(\frac{A_1}{A_2}\right) \quad (1)$$

2.2. Syntheses

2.2.1. [Re(bpy)(CO)$_3$(NO$_2$)] (**1**)

[Re(bpy)(CO)$_3$(CF_3SO_3)] (70 mg, 0.122 mmol) and 12-fold excess of $NaNO_2$ (101 mg, 1.46 mmol) were suspended in 15 mL of water. The mixture was heated at reflux for 2.5 h under Ar and protected from light. During that time a brilliant-yellow solid precipitated. The solid was filtered off, washed with water and dried under vacuum over P_4O_{10}. Yield: 51 mg (88%). Chem. *Anal.* Calc. for $C_{13}H_8N_3O_5Re$: C, 33.0; H, 1.7; N, 8.9. Found: C, 33.2; H, 1.7; N, 8.8%. ESIMS: *m*/*z* 495.99140 $(M+Na)^+$.

2.2.2. [Re(dmb)(CO)$_3$(ONO)] (**4**)

The synthesis was done with the same procedure as before from 100 mg of [Re(dmb)(CO)$_3$(CF_3SO_3)] (0.166 mmol) and 138 mg of $NaNO_2$ (2 mmol). Yield: 74 mg (90%) of a pale-yellow solid. Chem. *Anal.* Calc. for $C_{15}H_{12}N_3O_5Re$: C, 36.0; H, 2.4; N, 8.4. Found: C, 35.9; H, 2.3; N, 8.2%. ESIMS: *m*/*z* 524.02270 $(M+Na)^+$.

2.2.3. [Re(bpy)(CO)$_3$($^{15}NO_2$)] (**1′**) and [Re(dmb)(CO)$_3$($O^{15}NO$)] (**4′**)

The ^{15}N-labeled complexes were synthesized using a 6-fold excess of $Na^{15}NO_2$ with the same procedure for (**1**) and (**4**). The yields were 40% and 42% respectively. There were characterized by IR spectroscopy as it shows in Table 1.

2.3. X-ray structure determination

Yellow single crystals of complexes (**1**) and (**4**) were obtained by slow evaporation of acetone:water (1:1) solutions. These crystals were coated with perfluoropolyether, picked up with nylon loops and mounted in an Oxford Xcalibur, Eos, Gemini CCD area-detector diffractometer using graphite-monochromatic Mo Kα radiation (λ = 0.71073 Å) at 298 K. Final cell constants were obtained from least squares fits of several thousand strong reflections. Data was corrected for absorption with CrysAlisPro, Oxford Diffraction Ltd., Version 1.171.33.66, applying an empirical absorption correction using spherical harmonics, implemented in SCALE3 ABSPACK scaling algorithm [31]. The structures were solved by direct methods with SHELXS-97 and refined by full-matrix least-squares on F^2 with

Table 1
Relevant IR stretching frequencies in cm^{-1} for the nitro and nitrito complexes, including the ^{15}N-labeled complexes.

(**1**)[a]	(**1′**) [a]	(**4**) [a]	(**4′**) [a]	(**3**)[b]
2026 (νCO_{ax})		2016 (νCO_{ax})		2029 (νCO_{ax})
1926 (νCO_{eq})		1885 (νCO_{eq})		1919 (νCO_{eq})
1353 ($\nu_a NO_2^-$)	1326 ($\nu_a {}^{15}NO_2^-$)	1426 (νN = O)	1413 (ν^{15}N = O)	1357 (νNO_2^-)
1323 ($\nu_s NO_2^-$)	1297 ($\nu_s {}^{15}NO_2^-$)	1055 (νN–O)	1042 (ν^{15}N–O)	1322 ($\nu_s NO_2^-$)
810 (δONO)	804 ($\delta O^{15}NO$)	812 (δONO)	806 ($\delta O^{15}NO$)	–
568($\rho_w NO_2^-$)	562 ($\rho_w {}^{15}NO_2^-$)	–		

[a] Solid samples.
[b] Solution in CH_2Cl_2 (see the text for more details).

SHELXL-97 [32]. All non-hydrogen atoms were anisotropically refined and hydrogen atoms bound to carbon were placed at calculated positions and refined as riding atoms with isotropic displacement parameters.

In compound (**4**) structure, as a consequence of the crystallographic imposed two-folded axis, a static disorder between carbonyl ligand and the *trans* nitrito ligand, in a 0.5:0.5 ratio is observed. The only restraint applied within the two overlapping moieties of the disordered (carbonyl and nitrito ligands), was to the carbonyl oxygen atom, O2, and the nitrogen atom, N2, of the nitrito ligand which were refined roughly superposed (employing the EXYZ command) with equivalent fixed anisotropic displacement parameters (employing the EADP command). Additionally, the non-coordinated oxygen atom, O4, of the nitrito ligand component was modeled disordered around two positions in 0.5:0.5 ratio.

2.4. Quantum chemical calculations

The geometry optimizations, the vibrational frequencies and the electronic structures of nitro- and nitrite- isomers of complexes (**1**)–(**2**) and (**3**)–(**4**) were calculated by DFT methods using GAUSSIAN03 [33] program package. Calculations employed the hybrid Perdew, Burke, Ernzerhof exchange and correlation functional (PBE1PBE) [34]. For H, C, N and O atoms, 6-311G** basis set were used. The Re atom was described by quasirelativistic effective core pseudopotential and corresponding set of basic functions [35]. The solvent was described by conductor-like polarizable continuum model (CPCM) [36]. Excited singlet states (fifty states) were calculated by time-dependent DFT (TD-DFT). The UV–Vis absorption spectra were simulated with the GaussSum software [37], including all calculated transitions. Gaussian shapes (5500 cm^{-1} fwhm) of the absorption bands were assumed.

Chemical hardness (η), associated with the stability and reactivity of a chemical systems is approximated using Eq. (2). Electronic chemical potential (μ) is defined as the negative of electronegative of a molecule and is determined using Eq. (3). The global electrophilicity index (ω) introduced by Parr [30] is calculated using Eq. (4) and measures the capacity of a species to accept electrons.

$$\eta = \frac{(\varepsilon_{LUMO} - \varepsilon_{HOMO})}{2} \quad (2)$$

$$\mu = \frac{(\varepsilon_{HOMO} + \varepsilon_{LUMO})}{2} \quad (3)$$

$$\omega = \frac{\mu^2}{2\eta} \quad (4)$$

3. Results and discussion

3.1. Syntheses

The syntheses of the precursor complexes of Re(I) were performed according to literature [38] and those previously developed in our laboratory [39–43], starting from $[Re(CO)_5Cl]$ with slight modifications. The nitro and nitrito complexes (**1**) and (**4**) were prepared as solids with high yields by a modification of previously published procedure for Ru(II) complexes [44]. The purity of the complexes was confirmed by chemical analysis and mass spectrometry. The complexes were very soluble in acetone, dichloromethane and acetonitrile, slightly soluble in methanol and ethanol and insoluble in water. The nitro and nitrito complexes (**3**) and (**2**) were studied only in solution.

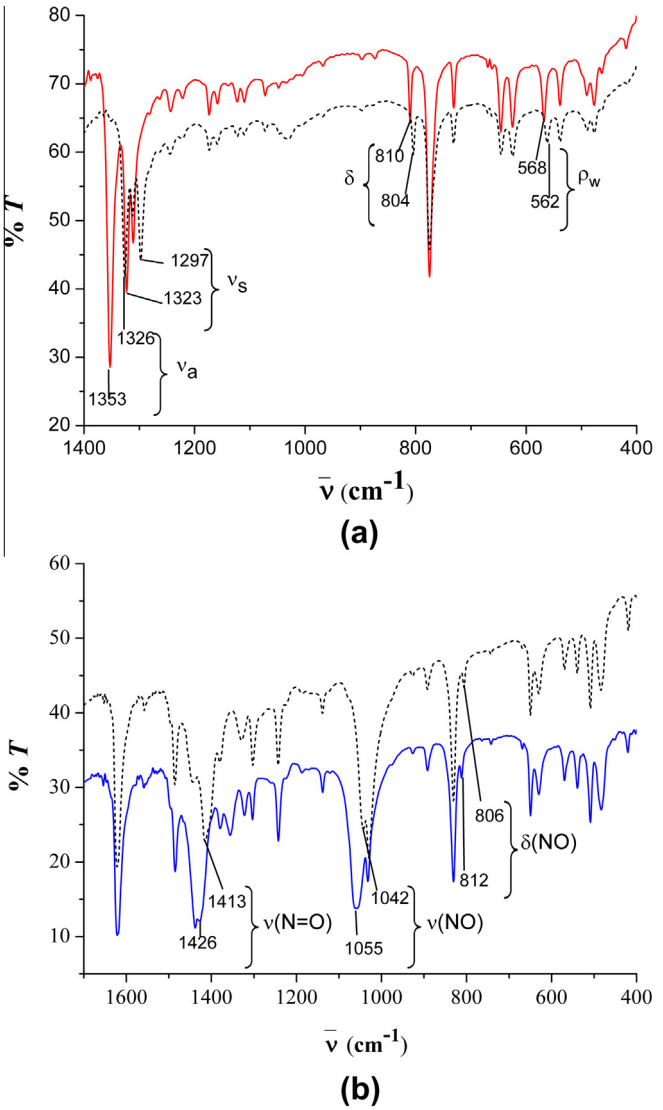

Fig. 1. IR spectra as KBr pellets of: (a) complex (**1**) (solid red line) and complex (**1′**) (dashed black line). (b) complex (**4**) (solid blue line) and complex (**4′**) (dashed black line). (Colour online.)

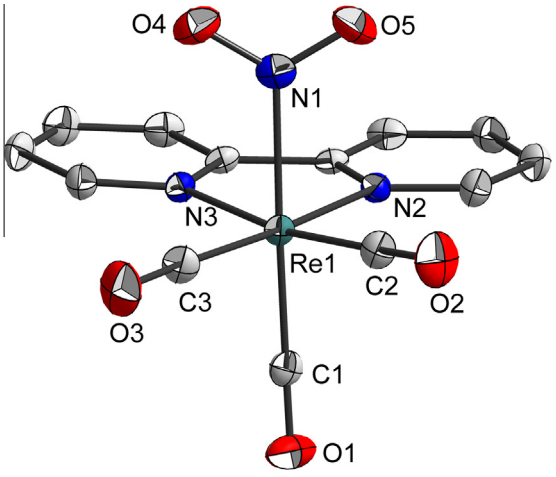

Fig. 2(a). ORTEP diagram for complex (**1**). Ellipsoid represents 50% of probability.

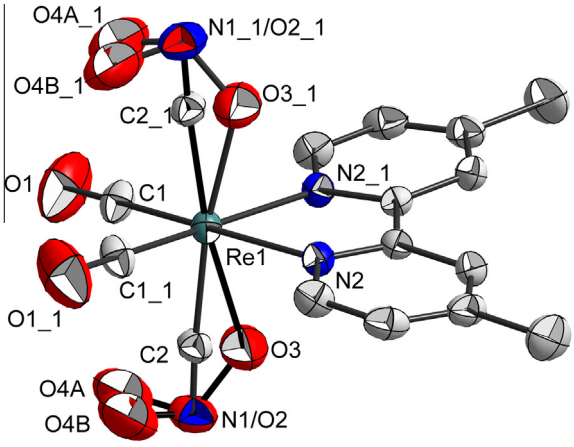

Fig. 2(b). ORTEP diagram for complex (**4**). Ellipsoid represents 50% of probability. The O4 was modeled disordered around two positions in a 0.5:0.5 ratio; 1:−*x*, *y*, 0.5 − *z*. (see the text for details).

3.2. IR spectra

The nitro and nitrito isomers are the most common forms in mononuclear complexes. When a crystal structure is not available, the isomers are usually differentiated by their IR spectra. For nitrito complexes, the two NO stretching frequencies ν(N═O) and ν(N–O) are well separated falling in the ranges 1510–1400 cm^{-1} and 1100–900 cm^{-1}, respectively. The separation is much smaller for the nitro complexes, which typically exhibit $\nu_a(NO_2)$ and $\nu_s(NO_2)$ bands in the ranges 1470–1370 cm^{-1} and 1340–1290 cm^{-1} respectively [45].

The IR spectra of complex (**1**) and (**4**) in KBr pellets (Fig. 1), display the characteristic vibrational modes for polypyridyl ligands between 1600 and 600 cm^{-1}. The values of the carbonyl stretching frequencies ($\nu_{C\equiv O}$) in a facial configuration for both complexes are almost the same as those reported for related complexes of the type *fac*-[Re(4,4′-X_2-bpy)$(CO)_3$(L)]PF_6 [39–43]. On the other hand, the values of the carbonyl stretching frequencies in (**1**) are higher (2026 and 1926 cm^{-1}) than those of (**4**) (2016 and 1885 cm^{-1}). The π-accepting capability is higher for bpy than for dmb and therefore there is π-backbonding from Re(I) to the carbonyl groups in (**1**) than in (**4**) [46] increasing the ($\nu_{C\equiv O}$) frequencies. In addition, a nitrite ion coordinated through the N atom is more electron withdrawing than when is coordinated through the O atom, contributing to the shifting of the carbonyl stretching frequencies to higher energies in complex (**1**). Table 1 gives the IR stretching frequencies for the new nitro and nitrito complexes, including the ^{15}N-labeled complexes. Based on the displacements between these

Table 2
Crystallographic refinement data for complexes (**1**) and (**4**).

Complex	(**1**)	(**4**)
Chemical formula	$C_{13}H_8N_3O_5Re$	$C_{15}H_{12}N_3O_5Re$
Crystal size (mm^3)	0.40 × 0.38 × 0.24	0.46 × 0.20 × 0.10
Formula weight	472.42	500.48
Lattice type	triclinic	monoclinic
Space group	$P\bar{1}$	$C2/c$
a (Å)	6.6337(3)	6.3927(2)
b (Å)	10.6572(5)	19.4344(6)
c (Å)	10.7531(5)	13.4758(6)
α (°)	79.675(4)	90.00
β (°)	73.366(4)	102,732(4)
γ (°)	72.074(4)	90.00
V (Å)	689.56(6)	1632.85(10)
Z	2	4
T (K)	298(2)	298(2)
ρ_{calcd} (g cm^{-3})	2.275	2.036
Reflection collected/$2\theta_{max}$	15716/54.00	8780/54.00
Unique reflection $I > 2\sigma(I)$	3014/2850	1777/1656
Number of parameters/restr.	199/0	126/1
λ (Å)/λ (Kα) (cm^{-1})	0.71073/8.84	0.71073/7.47
R1[a]/Goodness of fit[b]	0.0208/1.071	0.0243/1.077
wR_2 [c] ($I > 2\sigma(I)$)	0.0482	0.0556
Residual density (e $Å^{-3}$)	0.75/−1.22	0.75/−0.87

[a] Observation criterion: $I > 2\sigma(I)$ $R_1 = \sum||F_o| - |F_c||/\sum|F_o|$.

[b] GooF = $[\sum[w(F_o^2 - F_c^2)^2]/(n\text{-}p)]^{1/2}$.

[c] $wR_2 = [\sum[w(F_o^2 - F_c^2)^2]/\sum[w(F_o^2)^2]]^{1/2}$ where $w = 1/\sigma^2(F_o^2)+(aP)^2 + bP$, $P = (F_o^2 + 2F_c^2)/3$.

Table 3
Selected bond distances (Å) and angles (°) for (**1**) and (**4**).

(**1**)		(**4**)	
Bond lengths (Å)			
Re(1)–C(3)	1.913(4)	Re(1)–C(1)	1.906(5)
Re(1)–C(2)	1.917(4)	Re(1)–C(1_1)$^{\#}$	1.906(5)
Re(1)–C(1)	1.924(4)	Re(1)–C(2)	1.964(12)
Re(1)–N(2)	2.169(3)	Re(1)–C(2_1)$^{\#}$	1.964(12)
Re(1)–N(3)	2.169(3)	Re(1)–N(2)	2.169(3)
Re(1)–N(1)	2.181(3)	Re(1)–N(2_1)$^{\#}$	2.169(3)
N(1)–O(5)	1.232(5)	Re(1)–O(3)	2.089(8)
N(1)–O(4)	1.234(5)	Re(1)–O(3_1)$^{\#}$	2.089(8)
C(3)–O(3)	1.153(5)	N(1_1)–O(4A_1)	1.131(19)
C(2)–O(2)	1.144(5)	N(1)–O(4A)	1.332(10)
C(1)–O(1)	1.152(5)	C(1)–O(1)	1.154(6)
		C(1_1)–O(1_1)	1.154(6)
		C(2)–O(2)	1.120(2)
Bond angles (°)			
C(3)–Re(1)–C(2)	88.10(18)	C(1)–Re(1)–C(1_1)$^{\#}$	87.7(3)
C(3)–Re(1)–C(1)	88.00(18)	C(1)–Re(1)–C(2–1)$^{\#}$	86.3(4)
C(2)–Re(1)–C(1)	90.40(17)	C(1_1)$^{\#}$–Re(1)–C(2_1)$^{\#}$	84.1(4)
C(2)–Re(1)–N(2)	98.95(15)	C(1)–Re(1)–C(2)	84.1(4)
C(1)–Re(1)–N(2)	92.39(15)	C(1_1)$^{\#}$–Re(1)–C(2)	86.3(4)
C(3)–Re(1)–N(3)	98.21(15)	C(2_1)$^{\#}$–Re(1)–C(2)	166.7(6)
C(1)–Re(1)–N(3)	96.00(13)	C(1_1)$^{\#}$–Re(1)–N(2_1)$^{\#}$	172.65(16)
C(2)–Re(1)–N(3)	171.14(14)	C(1)–Re(1)–N(2_1)$^{\#}$	98.91(19)
N(2)–Re(1)–N(3)	74.73(11)	C(2_1)$^{\#}$–Re(1)–N(2_1)$^{\#}$	93.1(3)
C(3)–Re(1)–N(1)	94.90(16)	C(2)–Re(1)–N(2_1)$^{\#}$	97.5(3)
C(2)–Re(1)–N(1)	90.45(16)	N(2)–Re(1)–N(2_1)$^{\#}$	74.67(19)
C(1)–Re(1)–N(1)	177.00(14)	C(1)–Re(1)–O(3)	98.0(3)
N(2)–Re(1)–N(1)	84.64(12)	C(1_1)$^{\#}$–Re(1)–O(3)	103.1(3)
N(3)–Re(1)–N(1)	82.85(12)	O(3)–Re(1)–N(2)	77.5(3)
O(5)–N(1)–O(4)	118.7(4)	O(3)–Re(1)–N(2_2)$^{\#}$	79.3(3)
		O(4A)–N(1)–O(3)	111(3)

Symmetry transformations used to generate equivalent atoms: #1 −*x*, *y*, −*z* + 1/2.

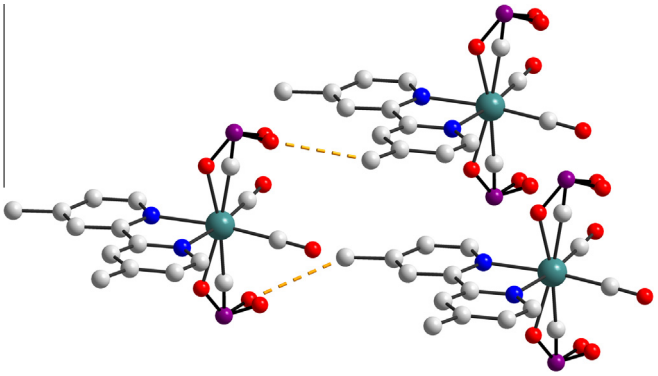

Fig. 3. The shortest interactions C–H···O–NO (nitrito) between the $-CH_3$ substituent in dmb and O-nitrite in complex (**4**).

Table 4
Electronic absorption data for complexes (**1**) to (**4**) in CH_2Cl_2 at 22 °C.

Complex	λ_{max}, nm ($10^{-3}\varepsilon_{max}$, M^{-1} cm^{-1})
(**1**)	369 (3.2), 318 sh (7.0), 286 (14.0), 244 (14.8)
(**2**)	382 (2.8), 292 (14.9), 255 sh (12.3), 240 (15.6)
(**3**)	356 (2.8), 314 sh (6.3), 280 (12.0), 250 (12.4)
(**4**)	372 (2.4), 290 (12.4), 256 (10.7), 238 (12.4)

bands we assign the frequencies (see Table 1) for that ligand in both complexes, and we have found that it is coordinated through N- in (**1**) (Fig. 1a) and through the O- in (**4**) (Fig 1b). This different linkage between both complexes has also been confirmed by X-ray structural determination, as seen in Figs. 2a and b.

In CH_2Cl_2, during the time of measurement (lesser than 5 min), the IR spectra of complexes (**1**) and (**4**) (Supplementary Figs. S1 and S2), evidence that in solution only (**4**) isomerizes to give the nitro complex, **[Re(dmb)(CO)$_3$(NO$_2$)]** (**3**), in agreement with other complexes with metals centers coordinated to nitrites [3] which suffer linkage isomerization processes. In (**3**), two new bands appear at 1357 and 1322 cm^{-1}, which can be assigned to asymmetric and symmetric stretching modes (ν_a and ν_s) respectively for this N-bond ligand (Table 1 and Supplementary Fig. S2). Additionally, the carbonyl bands shift to higher energies (2029 and 1919 cm^{-1}) respect to the solid sample (Supplementary Fig. S2), according with the better π-accepting capability of the nitro ligand respect to nitrito, as observed previously [47]. In contrast, for complex (**1**) the carbonyl frequencies and the bands corresponding to the nitro ligand are approximately the same than for the solid (Supplementary Fig. S1), showing that the nitro complexes are the most stable isomers in solution, as predicted by DFT calculations.

3.3. Crystal structure

Crystallographic data and values of R_1 and *wR* for crystals (**1**) and (**4**) are listed in Table 2. The ORTEP diagrams for complexes (**1**) and (**4**) are shown in Figs. 2a and b, while the main angles and distances are listed in Table 3. Finally, the crystal structures of (**1**) and (**4**), confirmed the different linkage of the nitrite ion in both complexes, predicted by IR spectroscopy. Both structures contain a distorted octahedron, although compound (**4**) present more deviations in the octahedron angles involving the nitrite ligand, considering that the only restraint applied was to the carbonyl oxygen atom, O2, and the nitrogen atom, N2, of the nitrito ligand which were refined roughly superposed with equivalent fixed anisotropic displacement parameters.

The distances Re–N (2,181(3) Å) for (**1**) and Re–O (2.089(8) Å) for complex (**4**), are similar to those found for nitro and nitrito complexes of Re(I) [47,48]. For (**1**), the N–O distances in the nitro ligand are approximately the same (1.233 Å), while for (**4**) the N–O distance in the nitrito for the uncoordinated oxygen N1–O4 is shorter (1.131(19) Å) than for the coordinated oxygen N1–O3 (1.332(10) Å), as expected due to its double bound character and accordingly with other nitrite complexes [47,48]. As already determined in polypyridyl tricarbonyl rhenium(I) species [43], in the

Table 5
Electrochemical data for complexes (**1**) and (**3**) in CH_2Cl_2 and CH_3CN at 100 mV/s vs. SCE.

Complex	Process	CH_2Cl_2		CH_3CN	
		$E_{1/2}$, V (ΔE, mV)	E_{peak} (V)	$E_{1/2}$, V (ΔE, mV)	E_{peak} (V)
(**1**)	$Re^{2+/+}$		1.54		1.56
	$bpy^{0/-}$	−1.32(105)		−1.22(96)	
	$Re^{+/0}$		−1.81		−1.66
(**3**)	$Re^{2+/+}$		1.51		1.53
	$dmb^{0/-}$	−1.40(103)		−1.32(84)	
	$Re^{+/0}$		–		1.81

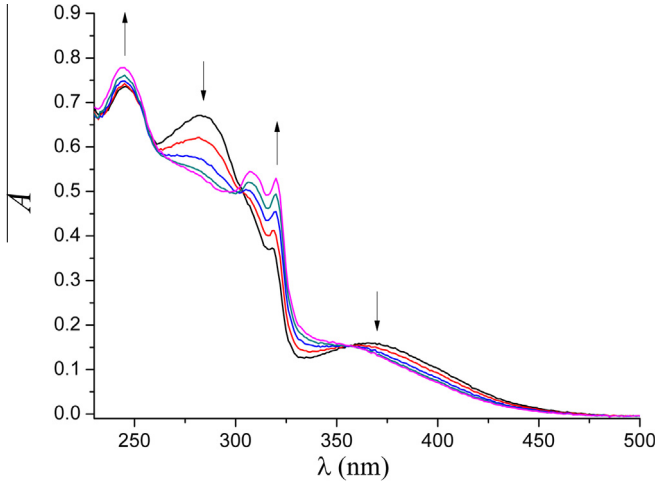

Fig. 4. Spectroelectrochemistry for complex (**1**) in 0.1 M $TBAPF_6$ in CH_2Cl_2. E = 1.55 V, t = 2 min, Δt = 0.4 min.

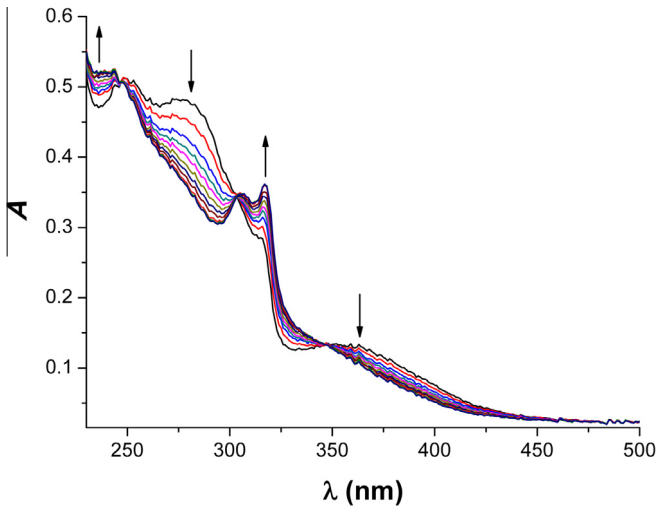

Fig. 5. Spectroelectrochemistry for complex (**3**) in 0.1 M $TBAPF_6$ in CH_2Cl_2. E = 1.55 V, t = 5 min, Δt = 0.4 min.

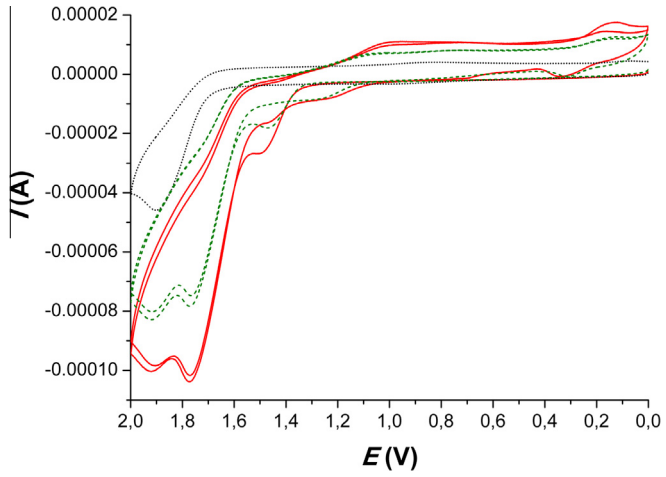

Fig. 6. Cyclic voltammetry at room temperature in CH_2Cl_2 – 0.1 M TBAH, $v = 100\ mVs^{-1}$ for: supporting electrolyte (dotted black line); complex (**1**) (solid red line); complex (**3**) (dashed green line). (Colour online.)

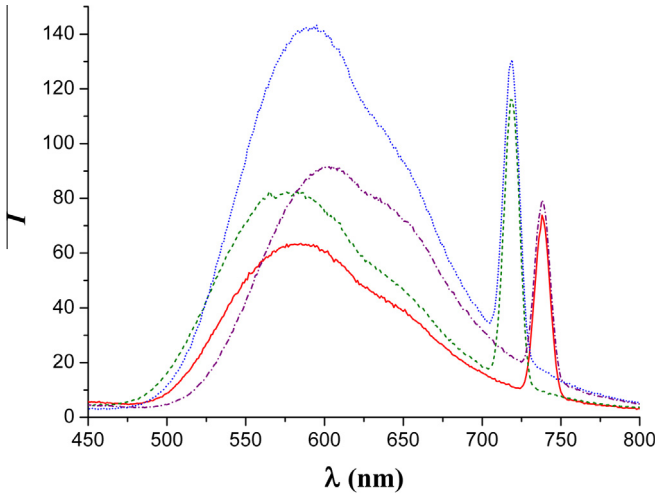

Fig. 7. Emission spectra for nitro complexes in CH_2Cl_2 before and after 50 min of irradiation for: complex (**1**) (solid red line); complex (**3**) (dashed green line), complex (**2**) (dashed dotted purple line) and complex (**4**) (dotted blue line). The peaks at 718 and 738 nm correspond to Rayleigh dispersion. λ_{irrad} = 369 nm for (**1**) and 359 nm for (**3**). (Colour online.)

crystal packing (Supplementary Figs. S3 and S4), the molecules present π–π stacking between adjacent bipirydyl ligands, the shortest plane to plane π–π distance between ring centroids have been estimated as 4.097–4.098 Å for complex (**1**), and 3.672–5.347 Å for complex (**4**). The shortest interactions C–H···O–NO (nitro) between bpy and N-nitrite was 2.6115(43) Å in complex (**1**), while in (**4**) exist C–H (methyl group)···O–NO (nitrito) interactions (between 2.4024(39) and 3.6677(43) Å) imposed by the $-CH_3$ substituent in dmb favoring the binding of the nitrite ion through oxygen as shown in Fig. 3. In both cases the experimental bond distances and angles are in good agreement with the values calculated using DFT as seen in Supplementary Table S5 and S6.

3.4. UV–Vis spectroscopy

Table 4 shows the electronic absorption data for complexes (**1**) to (**4**) in CH_2Cl_2. The bands between 200 and 320 nm can be assigned to characteristic intraligand $\pi \rightarrow \pi^*$ transitions of bpy or dmb. As in other Re(I) tricarbonyls polypyridines [39–43], the lowest energy bands for the nitro complexes at λ_{max} = 369 nm for (**1**) and λ_{max} = 356 nm in (**3**) are assigned to metal-to-ligand charge transfer transitions (MLCT) from the dπ orbital of Re to π* orbitals of bpy or dmb respectively. The shifting to higher energies for (**3**) is also related to the fact that electron donating $-CH_3$ substituents in dmb increase the energy of the π* (dmb) acceptor orbitals to a greater degree than to the dπ(Re) donor orbitals [46]. Moreover, in complexes (**2**) and (**4**) (obtained vide infra) the MLCT from the dπ orbital of Re to π* orbitals of bpy or dmb are shifted to lower energies (λ_{max} = 382 nm for (**2**) and λ_{max} = 372 nm in (**4**)), as expected in the nitrite ion in the O-nitrite binding mode, which is lesser π-accepting than the N-nitrite binding mode indicating the smaller HOMO–LUMO energy difference in the O-nitrite configuration.

3.5. Electrochemistry and spectroelectrochemistry

Table 5 shows the electrochemical data obtained from cyclic voltammetry for complexes (**1**) and (**3**) in CH_2Cl_2 and CH_3CN using 0.1 M $TBAPF_6$ as supporting electrolyte *versus* SCE. As related compounds the complexes displays in the oxidative region one irreversible oxidative wave associated with a metal centered reaction Re(I) → Re(II) and at least one reversible reduction wave assigned to the reduction of the polypyridine[38–43,46,49]. In CH_2Cl_2, for complexes (**1**) and (**3**) the redox potentials for the couple Re^{II}/Re^{I} appears at $E_{1/2}$ = 1.54 and 1.51 V, respectively, values very

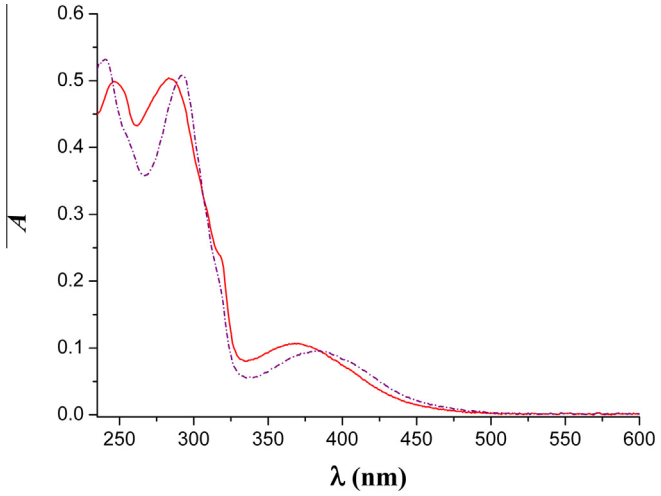

Fig. 8(a). UV–Vis spectra in CH_2Cl_2 for complex (**1**) before irradiation (solid red line) and after 50 min of irradiation at λ = 369 nm, complex (**2**) (dashed dotted purple line). (Colour online.)

similar to those reported for Meyer et al. [46]. As other polypyridines tricarbonyl Re(I) complexes [41,49], the first reduction wave based on the bipyridine ligand appears at $E_{1/2}$ = −1.32 for complex (**1**) and −1.40 V for complex (**3**), even as a second wave based in the couple Re^{I}/Re^{0} is observed at −1.81 V for (**1**) while for (**3**) this process is out of the electrochemical limits imposed by the solvent.

For complex (**3**) the dmb^0/dmb^- reduction occurs at more negative potentials than for (**1**) because the acceptor ability of the π* orbitals is diminished by the electron donating substituent. On the other hand, the reductant ability of the Re^{I} is increased in (**3**), as observed with the shifting to lower potentials for the Re^{II}/Re^{I} couple [46].

The oxidation based on the couple Re^{II}/Re^{I} was confirmed by controlled potential electrolyses for complexes (**1**) and (**3**) respectively. As shown in Figs. 4 and 5 when an external potential E = 1.55 V is applied for 2 or 5 min in the spectroelectrochemical cell to a 8.10^{-4} M solution of complex (**1**) or (**3**) in 0.1 M $TBAPF_6$ in CH_2Cl_2, the bleaching of the MLCT bands dπ(Re) → π*(bpy or

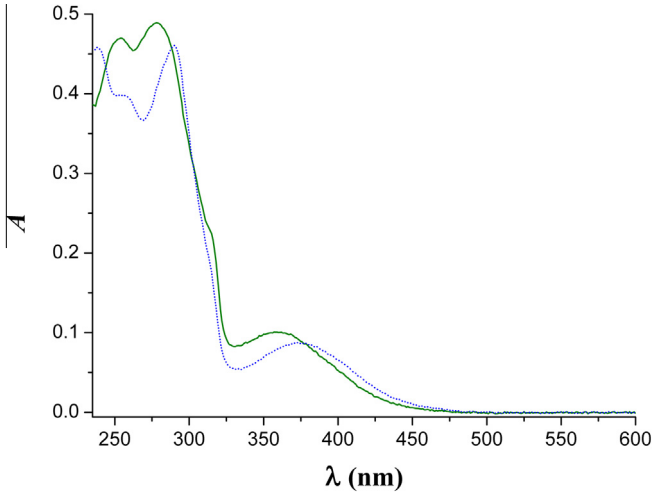

Fig. 8(b). UV–Vis spectra in CH_2Cl_2 for complex (**3**) before irradiation (solid green line) and after 50 min of irradiation at λ = 359 nm, complex (**4**) (dotted blue line). (Colour online.)

Table 6
DFT PBE1PBE/CPCM-CH_2Cl_2 calculated energies (eV) and compositions of selected highest occupied and lowest unoccupied molecular orbitals expressed in terms of composing fragments for complexes (**1**) to (**4**).

Complex	MO	*E* (eV)	Re	CO_{ax}	CO_{eq}	NO_2/ONO	bpy/dmb
1	LUMO+1	−1.6	1	0	2	0	96
	LUMO	−2.57	3	0	3	1	92
	HOMO	−6.72	54	9	15	17	5
	HOMO−1	−6.79	64	14	13	3	7
	HOMO−2	−6.91	38	6	11	42	3
2	LUMO+1	−1.62	1	0	1	0	97
	LUMO	−2.59	2	0	3	1	94
	HOMO	−6.46	59	15	13	8	4
	HOMO−1	−6.5	44	6	9	33	7
	HOMO−2	−6.86	58	8	20	12	2
3	LUMO+1	−1.46	2	0	2	0	96
	LUMO	−2.45	3	0	3	1	93
	HOMO	−6.66	54	9	15	14	7
	HOMO−1	−6.72	63	14	12	3	8
	HOMO−2	−6.86	38	6	12	41	3
4	LUMO+1	−1.46	1	0	1	0	97
	LUMO	−2.49	2	0	3	1	94
	HOMO	−6.41	59	15	13	8	5
	HOMO−1	−6.44	45	7	9	31	8
	HOMO−2	−6.81	58	7	21	11	2

dmb) is observed as a consequence of the oxidation centered in the Re(I). The presence of isosbestic points at 296, 302 and 358 nm for complex (**1**) and at 247, 303 and 347 nm for complex (**3**), suggests the absence of other processes [50]. When a potential of 0 V was applied in both cases the complexes are recovered in 85%. On the other hand, for complexes (**1**) and (**3**) applying an external potential of 1.8 V results in the loss of isosbestic points and definition of the spectrum in agreement with decomposition of the complexes.

As observed previously for ruthenium [5–8,51] osmium [52] and iron [53] complexes, the coordinated nitrite ion is unstable and disproportionate upon oxidation producing the corresponding nitrosyl and nitrato complexes. This disproportionation can also be observed in complex (**1**) and (**3**) by cyclic voltammetry scanning to higher positive potentials between 0.0 and 2.0 V. As seen in Fig. 6, for both complexes, an irreversible oxidation wave appears around 1.84 V and a reversible reduction at $E_{1/2}$ = 0.24 V, which can be assigned to the reversible nitrosyl couple, as well as the first oxidation wave at ~1.54 V disappear in concordance with mechanism proposed for nitro complexes of polypiridyl ruthenium(III) [5].

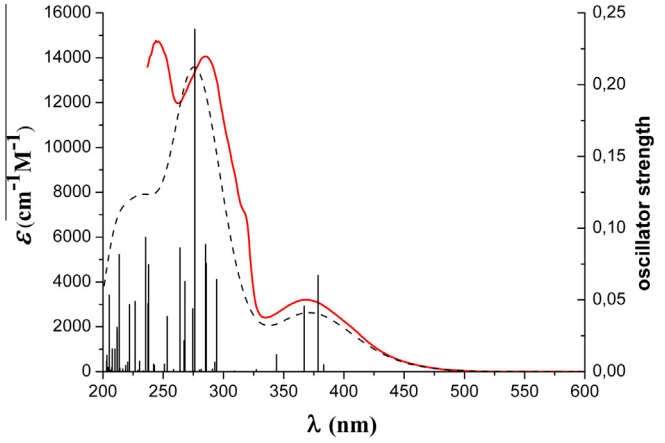

Fig. 9(a). UV–Vis spectra for complex (**1**) in CH_2Cl_2, experimental (solid red line) and calculated by TD-DFT (black dash line). (Colour online.)

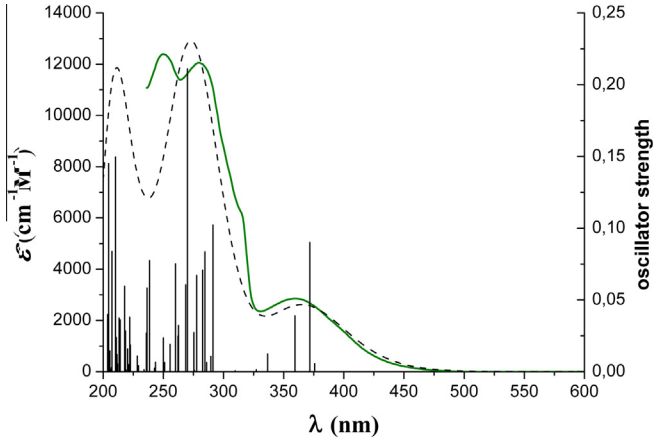

Fig. 9(b). UV–Vis spectra for complex (**3**) in CH_2Cl_2, experimental (solid green line) and calculated by TD-DFT (black dash line). (Colour online.)

We thus confirm that the coordinated nitrite ion through the N-atom is unstable and disproportionate upon oxidation involving isomerization of the nitrite ligand as observed previously for other metal complexes [51–53]. Work in progress will be done to identify the products of this reaction.

Besides, in CH_3CN solutions protected from light (to avoid the solvation of the complex, vide infra), both complexes suffer decomposition after oxidation generating the acetonitrile complexes. The cyclic voltamogramms of complexes (**1**) and (**3**) in CH_3CN present in the oxidative region two waves. The first one assigned to rhenium-based oxidation in the nitro complexes (as seen in Table 5) and the second one at *E* = 1.89 V and *E* = 1.85 V corresponding to the couple Re^{II}/Re^{I} in the electrogenerated acetonitrile complexes $[Re(bpy)(CO)_3(CH_3CN)]^+$ and $[Re(dmb)(CO)_3(CH_3CN)]^+$ respectively. In the negative potentials region two waves appear that can be assigned to bipyridine-based and rhenium-based reductions. This decomposition after oxidation was observed previously in similar rhenium(I) complexes [54–56] and in this work was confirmed by comparison with voltammograms of the synthesized acetonitrile complex $[Re(dmb)(CO)_3(CH_3CN)]^+$ [1]and with values reported in the literature for both complexes [38a,57].

[1] The $[Re(dmb)(CO)_3(CH_3CN)]^+$ as ClO_4- salt was obtained as solid state from $[Re(dmb)(CO)_3(NO_2)]^+$ using CH_3CN/H_2O (1:1 v/v) as solvent. Yield: 78%. Chem. *Anal.* Calc. for $C_{17}H_{15}N_3O_7Re$: C, 34.3; H, 2.5; N, 7.1. Found: C, 34.5; H, 2.5; N, 7.2%.

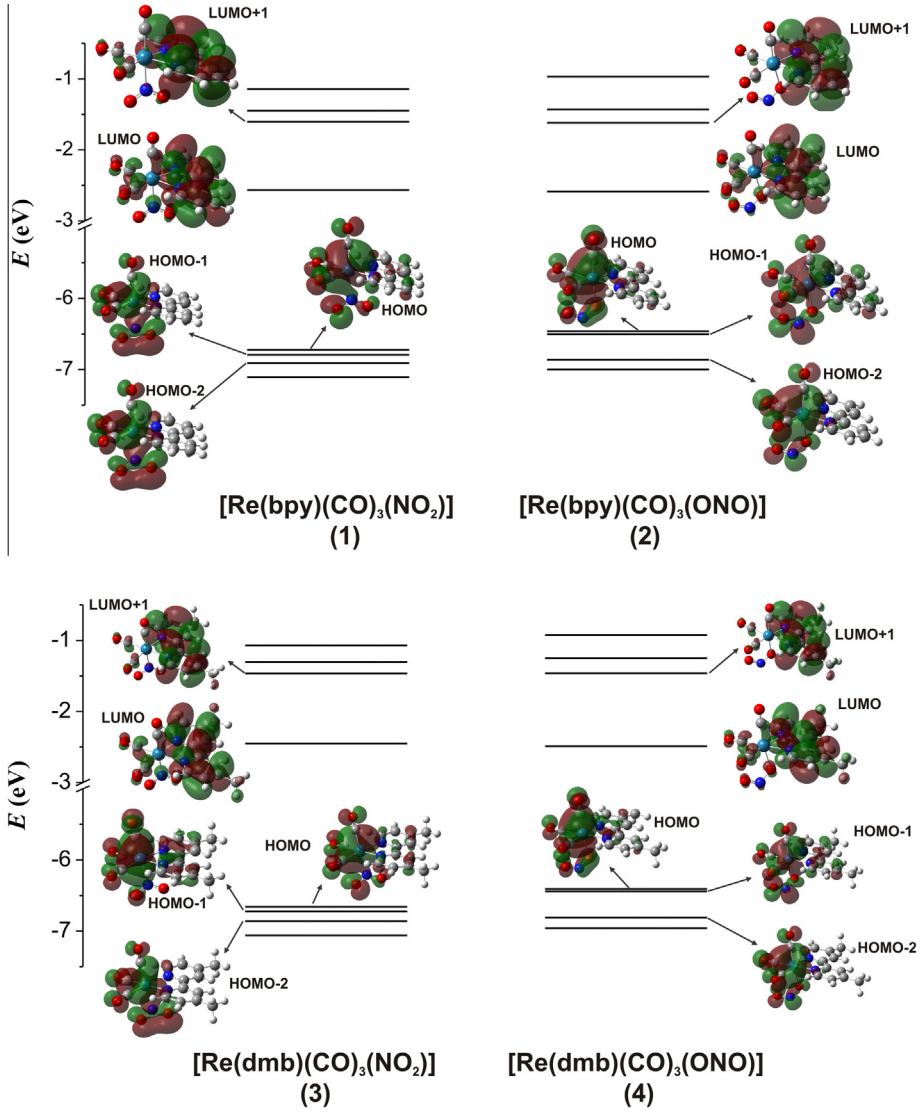

Fig. 10. DFT PBE1PBE/CPCM-CH_2Cl_2 energy level diagrams for complexes (**1**), (**2**), (**3**) and (**4**). Forms and approximate description of the frontier orbitals are included.

3.6. Luminescence and photolysis

As shown in Fig. 7, the nitro complexes emit weakly at room temperature in CH_2Cl_2 solutions when are irradiated at λ_{irrad} = (369 ± 10 nm). Complex (**1**) emits at λ_{em} = 581 nm while (**3**) at λ_{em} = 566 nm. The shifting to the red for the nitro complex is in concordance with the lower energy difference between states involve in the MLCT transition for that complex, which was also observed in the electronic absorption spectra (Figs. 8a and b). The luminescence quantum yields for both complexes have been determined as Φ = 0.0016 for (**1**) and Φ = 0.0012 for (**3**) using $[Ru(bpy)_3]^{2+}$ in CH_2Cl_2 as standard and corrected by absorbance (Φ = 0.029 [58]) in agreement with other diimine tricarbonyl Re(I) complexes studies in our group.[39–43].

The linkage isomerization by effect of light was observed previously for nitrite complexes of ruthenium [59], cobalt [60,61] and manganese [62]. In this sense, after 50 min of irradiation for both complexes, a displacement of the emission bands to lower energy (λ_{max} = 605 nm for (**1**) and 592 nm for (**3**)) and an increment in the intensity of emission was observed as seen in Fig. 7, which is in agreement with the isomerization of complex (**1**) and (**3**) to give the nitrito complexes **[Re(bpy)(CO)$_3$(ONO)]** (**2**) and (**4**) respectively. From the spectral changes, the isomerization rate constants at room temperature were estimated as $\sim 10^{-3}$ s^{-1} for both complexes; which is 2.8 times higher than *cis*-$[Co(en)_2(CN)(ONO)]^+$ [2] due to the higher π-accepting capability of carbonyls group and bpy or dmb in these complexes. Moreover, the UV–Vis spectrum for complexes (**1**) and (**3**) after irradiation shows that in both cases the MLCT bands shift to higher wavelengths (Figs. 8a and b). The decrease in the energy of the MLCT due to the nitrite ion in the O-nitrite binding mode is $\Delta E \sim 1190$ cm^{-1}, in agreement with the lesser π-accepting ability than in the N-nitrite binding mode.

On the other hand, in CH_3CN solutions, both complexes suffer a light-induced solvation process to give the corresponding acetonitrile complexes, as evidenced by the increment of the intensity of emission at wavelengths characteristics of these CH_3CN complexes with time of irradiation and by the final UV–Vis spectra. Supplementary Figs. S7(a) and S8(a) shows changes of emission after irradiation for 3 h, at λ_{irrad} = 353 nm for (**1**) and λ_{irrad} = 347 nm for (**3**). The increments in the emission intensity with time allow us to estimate the pseudo-first order constants for the photosubstitution reactions of the nitrite ligand by acetonitrile (Supplementary Fig. S7(b) and S8(b)), giving a value of $k = 5.6.10^{-4}$ s^{-1} for (**1**) and

Table 7
Global chemical reactivity indices for complexes (**1**)–(**4**).

Complex	**1**	**2**	**3**	**4**
ΔE (eV)	4.15	*3.87*	*4.21*	*3.92*
η (eV)	2.075	1.935	2.105	1.96
μ (eV)	−4.645	−4.525	−4.555	−4.45
ω (eV)	5.199	5.291	4.928	5.052

$k = 5.8.10^{-4}\ s^{-1}$ for (**3**). In ethanol/water (2:1) solutions, the complexes also decompose to give the corresponding acuo complexes which were confirmed by chemical analyses, UV–Vis, IR spectroscopy and crystal structure.

3.7. Computational calculations

Table 6 shows selected DFT calculated energies and compositions of selected orbitals expressed in terms of composing fragments. Figs. 9a and 9b shows the experimental and calculated UV–Vis absorption spectra for complex (**1**) and (**3**) in CH_2Cl_2, while Supplementary Table S9 summarized the TD-DFT calculated energies of low-lying singlet electronic transitions for complexes (**1**)–(**4**), the oscillator strengths and experimental values. Moreover, Fig. 10 shows the molecular orbital diagrams for complexes (**1**)–(**4**). It could be seen that the LUMO and LUMO+1 are π^* orbitals primarily localized on the bipyridine ligands for all complexes. The energies of these orbitals are approximately the same for isomers, (**1**)–(**2**) and (**3**)–(**4**), while for the same isomer between bpy and dmb complexes it could be observed the increase of energy of the orbitals for the dmb complex in agreement with the trend observed experimentally (Figs. 8a and b, Table 4 and 5). On the other hand, the HOMO is predominantly based in dπ orbitals of the Re atom. In the nitro complexes (**1**) and (**3**), it has a contribution of the nitrite ligand, while for complexes (**2**) and (**4**) it has a contribution of the axial CO. The HOMO−1 is also a rhenium based orbital, with a contribution of the nitrite ligand for complexes (**2**) and (**4**) and with a contribution of the CO axial for complexes (**1**) and (**3**), inversely than for the previous case. Besides the HOMO−2 is a Re and nitrite based orbital for complexes (**1**) and (**3**), while for complexes (**2**) and (**4**) the contribution of nitrite to this orbital is minor (Table 6). These differences could explain the difference in energy of the orbitals between isomers, giving as a result the decrease on the energy for the transitions for the nitrito complexes, in agreement with the trend observed experimentally for the electronic absorption (Figs. 9a and b) and emission spectra (Fig. 7). The calculated difference energy ($\Delta E \sim 0.9$ kJ mol^{-1}) between isomers (**1**)–(**2**) and (**3**)–(**4**) in CH_2Cl_2 gave the nitro isomers as the lowest energy structure, in agreement with UV–Vis and IR spectra in CH_2Cl_2 (Figs. 8a and b and Supplementary Figs. S1 and S2) for both complexes.

At the same time as the chemical reactivity descriptors calculated using DFT for the isomers (**1**)–(**4**) in CH_2Cl_2 (Table 7) predict that in both cases the nitro isomers (complexes (**1**) and (**3**)) are the more stables and less reactive. Furthermore, the electrophilicity values followed the hardness trend of the minimum electrophilicity principle (MEP), "more stable isomers correspond to lesser electrophilicity values". As shown in Table 7 the electrophilicity index (ω) between isomers (**1**)–(**2**) and (**3**)–(**4**) decreases from the nitro isomers to the nitrite isomers. In addition the electrophilicity index is higher for complex (**3**) than for complex (**1**), an indication of reduction of π-backbonding ability of the dmb than bpy due to the introduction of the $-CH_3$ group in agreement with IR and UV–Vis spectra in CH_2Cl_2. Along with the electronic chemical potential trend is (**4**) > (**2**) > (**3**) > (**1**).

Figs. 9a and b shows a good agreement with the experimental and calculated electronic spectra of complexes (**1**) and (**3**) in CH_2Cl_2 although the molar absorptivities are overestimated. As seen in Supplementary Table S9, two allowed electronic transitions were calculated to contribute to the lowest energy absorption band. For (**1**) and (**3**) these transitions correspond to HOMO → LUMO which is MLCT, and HOMO−2 → LUMO that can be described as mixed MLCT/LLCT (ligand-to-ligand charge transfer) with participation of the nitrite ion [40–43] or as MLLCT (metal–ligand-to-ligand charge transfer), as found previously in similar Re(I) tricarbonyl complexes and suggested experimentally [63]. For nitrito complexes, (**2**) and (**4**), the two main electronic transitions that contribute to the lowest energy band correspond to HOMO−1 → LUMO, described as MLLCT, and HOMO → LUMO, described as MLCT.

4. Conclusions

We have synthesized, characterized, determined their physicochemical properties and solved the crystal structures by X-ray diffraction of two new tricarbonyl rhenium(I) complexes with different polypyridyl ligands in the coordination sphere and coordinated to the nitrite ion in the N- and O-binding mode. In this way we made a contribution to understand the factors that controls the occurrence of different isomers in nitrite complexes, which have relevance related with the biological properties of this anion coordinated to metalloproteins. In this context, we have found that as solid the different binding mode could be explained due to the different steric requirements of both polipyridines employed as ancillary ligands. We have found that complex (**1**) as solid exist as N-binding mode because exist C–H···O–NO (nitro) interactions between bpy and N-nitrite, while in complex (**4**) the $-CH_3$ substituents in dmb imposed the C–H (methyl group)···O–NO (nitrito) interactions favoring the O-binding mode. In contrast, in CH_2Cl_2 solution, only complex (**4**) rapidly isomerizes to the N-nitrite form, illustrating the small differences of energy between both isomers. These experimental studies on Re(I) tricarbonyls have been accompanied with density functional theory (DFT) calculations and shows that nitro and nitrito linkage isomers (**1**)–(**2**) and (**3**)–(**4**) have similar energies, being the nitro isomer the most stable and lesser reactive in CH_2Cl_2 in both cases. Furthermore, by DFT and TD-DFT calculations we have confirmed the assignment of the electronic transitions and the nature of the orbitals involved. Finally, we have found that both complexes present isomerization induced by light and presumably by electrochemical oxidation, which can be used in the design of new materials or as synthetic precursors for nitrosyl compounds and which have relevance related with the biological properties of this anion coordinated to metalloproteins.

Acknowlegments

We thank Universidad Nacional de Tucumán (UNT), Consejo Nacional de Investigaciones Científicas y Técnicas (CONICET), and Agencia Nacional de Promoción Científica y Tecnológica (ANPCyT), all from Argentina, for financial support. F.F. and P.A. are Members of the Research Career from CONICET. S.E.D. thanks CONICET for a graduate fellowship. We also thank Dr. Fabio Doctorovich (INQUIMAE, UBA) for giving us $Na^{15}NO_2$ and Dr. Néstor E. Katz (INQUINOA, UNT) for helpful discussions.

Appendix A. Supplementary data

CCDC 916047 and 916048 contains the supplementary crystallographic data for **[Re(bpy)(CO)$_3$(NO$_2$)]** and **[Re(dmb)(CO)$_3$(ONO)]**. These data can be obtained free of charge via http://www.ccdc.cam.ac.uk/conts/retrieving.html, or from the Cambridge Crystallographic Data Centre, 12 Union Road, Cambridge CB2 1EZ, UK; fax:

(+44) 1223-336-033; or e-mail: deposit@ccdc.cam.ac.uk. Supplementary data associated with this article can be found, in the online version, at http://dx.doi.org/10.1016/j.poly.2013.10.002.

References

[1] N.N. Greenwood, A. Earnshaw, Chemistry of the Elements, second ed., School of Chemistry University of Leeds, UK, 1997. 463.
[2] (a) K. Miyoshi, N. Katoda, H. Yoneda, Inorg. Chem. 22 (1983) 1839;
(b) A. Eslami, Therm. Acta 409 (2004) 189;
(c) I. Ciofini, C. Adamo, J. Phys. Chem. A 105 (2001) 1086.
[3] J. Heinecke, P.C. Ford, Coord. Chem. Rev. 254 (2010) 235.
[4] D.M.L. Goodgame, M.A. Hitchman, Inorg. Chem. 3 (1964) 1389.
[5] D.A. Freedman, S. Kruger, C. Roosa, C. Wymer, Inorg. Chem. 45 (2006) 9558.
[6] F.R. Keene, D.J. Salmon, J.L. Walsh, H.D. Abruña, T.J. Meyer, Inorg. Chem. 19 (1980) 1896.
[7] R.A. Leising, S.A. Kubow, L.F. Szczepura, K. Takeuchi, J. Inorg. Chim. Acta 245 (1996) 167.
[8] H. Nagao, M. Mukaida, K. Shimizu, F.S. Howell, H. Kakihana, Inorg. Chem. 25 (1986) 4312.
[9] H. Nagao, H. Nishimura, Y. Kinataka, F.S. Howell, M. Mukaida, L. Kanihana, Inorg. Chem. 29 (1990) 1693.
[10] P. Coppens, I. Novozhilova, A. Kovalevsky, Chem. Rev. 102 (2002) 861.
[11] (a) M.S. Thompson, T.J. Meyer, J. Am. Chem. Soc. 103 (1981) 5577;
(b) W.R. Murphy Jr., K.J. Takeuchi, T.J. Meyer, J. Am. Chem. Soc. 104 (1982) 5817.
[12] W.R. Murphy Jr., K. Takeuchi, M.H. Barley, T.J. Meyer, Inorg. Chem. 25 (1986) 1041.
[13] M. Feelish, B.O. Fernandez, N.S. Bryan, M.F. Garcia-Saura, S. Bauer, D.R. Whitlock, P.C. Ford, D.R. Janero, J. Rodriguez, H. Ashrafian, J. Biol. Chem. 283 (2008) 33927.
[14] K. Cosby, K.S. Partovi, J.H. Crawford, R.P. Patel, C.D. Reiter, S. Martyr, B.K. Yang, M.A. Waclawiw, G. Zalos, X. Xu, K.T. Huang, H. Shields, D.B. Kim-Shapiro, A.N. Schechter, Nat. Med. 9 (2003) 1498.
[15] S. Shiva, M.N. Sack, J.J. Greer, M. Duranski, L.A. Ringhood, L. Burwell, X. Wang, P.H. MacArthur, A. Shoja, N. Raghavachari, J.W. Calvert, P.S. Brookes, D.J. Lefer, M.T. Gladwin, J. Exp. Med. 204 (2007) 2089.
[16] M. Mazzone, P. Carmeliet, Nature 453 (2008) 1194.
[17] M.T. Gladwin, Nat. Chem. Biol. 1 (2005) 245.
[18] N.S. Bryan, B.O. Fernandez, S.M. Bauer, M.F. Garcia-Saura, A.B. Milsom, T. Rassaf, R.E. Maloney, Nat. Chem. Biol. 1 (2005) 290.
[19] K.T. Huang, A. Keszler, N. Patel, R.P. Patel, M.T. Galddwin, D.B. Kim-Shapidro, N. Hogg, J. Biol. Chem. 280 (2005) 31126.
[20] R. Grubina, Z. Huang, S. Shiva, M.S. Joshi, I. Azarov, S. Basu, L.A. Ringwood, A. Jiang, N. Jogg, D.B. Kim-Shapiro, M.T. Gladwin, J. Biol. Chem. 282 (2007) 12916.
[21] B.O. Fernandez, I.M. Lorkovic, P.C. Ford, Inorg. Chem. 42 (2003) 2.
[22] B.O. Fernandez, P.C. Ford, J. Am. Chem. Soc. 125 (2003) 10510.
[23] P.C. Ford, Inorg. Chem. 49 (2010) 6226.
[24] D.M. Copeland, A.S. Soares, A.H. West, G.B. Richter-Addo, J. Inorg. Biochem. 100 (2006) 1413.
[25] J. Yi, M.K. Safo, G.B. Richter-Addo, Biochemistry 47 (2008) 8247.
[26] J. Yi, J. Heinecke, H. Tan, P.C. Ford, G.B. Richter-Addo, J. Am. Chem. Soc. 131 (2009) 18119.
[27] R. Silaghi-Dumitrescu, Inorg. Chem. 43 (2004) 3715.
[28] L.L. Perissinotti, M.A. Marti, F. Doctorovich, F.J. Luque, D.A. Estrin, Biochemistry 47 (2008) 9793.
[29] N. Xu, J. Yi, G.B. Richter-Addo, Inorg. Chem. 49 (2010) 6253.
[30] R.G. Parr, L.v. Szentpály, S. Liu, J. Am. Chem. Soc. 121 (1999) 1922;
(a) C.A. Mebi, J. Chem. Sci. 123 (2011) 727;
(b) S. Pan, M. Solà, P.k. Chattaraj, J. Phys. Chem. A 117 (2013) 1843.
[31] SCALE3 ABSPACK: Empirical absorption correction, CrysAlis – Software package, Oxford Diffraction Ltd., Oxford, 2006.
[32] G.M. Sheldrick, SHELXS97 and SHELXL97, Programs for Crystal Structure Resolution, University of Göttingen, Göttingen, Germany, 1997.
[33] Gaussian 03, Revision C.02, M.J. Frisch, G.W. Trucks, H.B. Schlegel, G.E. Scuseria, M.A. Robb, J.R. Cheeseman, J.A. Montgomery, Jr., T. Vreven, K.N. Kudin, J.C. Burant, J.M. Millam, S.S. Iyengar, J. Tomasi, V. Barone, B. Mennucci, M. Cossi, G. Scalmani, N. Rega, G.A. Petersson, H. Nakatsuji, M. Hada, M. Ehara, K. Toyota, R. Fukuda, J. Hasegawa, M. Ishida, T. Nakajima, Y. Honda, O. Kitao, H. Nakai, M. Klene, X. Li, J.E. Knox, H.P. Hratchian, J.B. Cross, C. Adamo, J. Jaramillo, R. Gomperts, R.E. Stratmann, O. Yazyev, A.J. Austin, R. Cammi, C. Pomelli, J.W. Ochterski, P.Y. Ayala, K. Morokuma, G.A. Voth, P. Salvador, J.J. Dannenberg, V.G. Zakrzewski, S. Dapprich, A.D. Daniels, M.C. Strain, O. Farkas, D.K. Malick, A.D. Rabuck, K. Raghavachari, J.B. Foresman, J.V. Ortiz, Q. Cui, A.G. Baboul, S. Clifford, J. Cioslowski, B.B. Stefanov, G. Liu, A. Liashenko, P. Piskorz, I. Komaromi, R.L. Martin, D.J. Fox, T. Keith, M.A. Al-Laham, C.Y. Peng, A. Nanayakkara, M. Challacombe, P.M. W. Gill, B. Johnson, W. Chen, M.W. Wong, C. Gonzalez, J. A. Pople, Gaussian Inc., Wallingford CT, 2004.
[34] (a) P. Perdew, K. Burke, M. Ernzerhof, Phys. Rev. Lett. 77 (1996) 3865;
(b) C. Adamo, J. Barone, J. Chem. Phys. 110 (1999) 6158.
[35] (a) D. Andrae, U. Haeussermann, M. Dolg, H. Stoll, H. Preuss, Theor. Chim. Acta 77 (1990) 123;
(b) J.M.L. Martin, A. Sundermann, J. Chem. Phys. 114 (2001) 3408.
[36] M. Cossi, N. Rega, G. Scalmani, V. Barone, J. Comput. Chem. 24 (2003) 669.
[37] N.M. O'Boyle, A.L. Tenderholt, K.M. Langner, J. Comput. Chem. 29 (2008) 839.
[38] (a) J.V. Caspar, T.J. Meyer, J. Phys. Chem. 87 (1983) 952;
(b) J.K. Hino, L. Della Ciana, W.J. Dressick, B.P. Sullivan, Inorg. Chem. 31 (1992) 1072;
(c) L. Sacksteden, A.P. Zipp, E.A. Brown, J. Streich, J.N. Demas, B.A. DeGraff, Inorg. Chem. 29 (1990) 4335.
[39] (a) F. Fagalde, N.E. Katz, J. Coord. Chem. 54 (2001) 367;
(b) M.G. Mellace, F. Fagalde, N.E. Katz, Polyhedron 22 (2003) 369;
(c) N.E. Katz, S.L. Mecklemburg, T.J. Meyer, Inorg. Chem. 35 (1995) 1282.
[40] M. Cattaneo, F. Fagalde, N.E. Katz, Inorg. Chem. 45 (2006) 6884.
[41] M. Cattaneo, F. Fagalde, N.E. Katz, A.M. Leiva, R. Schmehl, Inorg. Chem. 45 (2006) 127.
[42] M. Cattaneo, F. Fagalde, N.E. Katz, C.D. Borsarelli, T. Parella, Eur. J. Inorg. Chem. 34 (2007) 5323.
[43] G. Pourrieux, F. Fagalde, M.I. Romero, X. Fontrodona, T. Parella, N.E. Katz, Inorg. Chem. 49 (2010) 4084.
[44] M. Videla, J.S. Jacinto, R. Baggio, M.T. Garland, P. Singh, W. Kaim, L.D. Slep, J.A. Olabe, Inorg. Chem. 45 (2006) 8608.
[45] K. Nakamoto, Infrared and Raman Spectra of Inorganic and Coordination Compounds, fourth ed., Wiley, New York, 1986. p. 221.
[46] L.A. Worl, R. Duesing, P. Chen, L. Della Ciana, T.J. Meyer, J. Chem. Soc., Dalton Trans. (1991) 849.
[47] B.F.G. Johnson, A. Sieker, A.J. Blake, R.E.P. Winpenny, J. Organomet. Chem. 475 (1994) 193.
[48] A. Sieker, A.J. Blake, B.F.G. Johnson, J. Chem. Soc., Dalton Trans. (1996) 1419.
[49] R. Lin, Y. Fu, C.P. Brock, T.F. Guarr, Inorg. Chem. 31 (1992) 4346.
[50] R.G. Wilkins, Kinetics and Mechanism of Transition Metal Complexes, second ed., VCH, Weinheim, 1991, p. 156.
[51] F.R. Keene, D.J. Salmon, T.J. Meyer, J. Am. Chem. Soc. 99 (1977) 2384.
[52] D.W. Pipes, T.J. Meyer, Inorg. Chem. 23 (1984) 2466.
[53] M.G. Finnegan, A.G. Lappin, W.R. Scheidt, Inorg. Chem. 29 (1990) 181.
[54] F. Paolucci, M. Marcaccio, C. Paradisi, S. Roffia, C.A. Bignozzi, C. Amatore, J. Phys. Chem. B 102 (1998) 4759.
[55] J.P. Bullock, E. Carter, R. Johnson, A.T. Kennedy, S.E. Key, B.J. Kraft, D. Saxon, P. Underwood, Inorg. Chem. 47 (2008) 7880.
[56] P. Christensen, A. Hamnett, A.V.G. Muir, J.A. Timney, J. Chem. Soc., Dalton Trans. (1992) 1455.
[57] J.R. Shaw, R.H. Schmehl, J. Am. Chem. Soc. 113 (1991) 389.
[58] J.V. Caspar, T.J. Meyer, J. Am. Chem. Soc. 105 (1983) 5583.
[59] D. Schaniel, N. Mockus, T. Woike, A. Klein, D. Sheptyakov, T. Todorova, B. Delley, Phys. Chem. Chem. Phys. 12 (2010) 6171.
[60] V. Balzani, R. Ballardini, N. Sabbatini, L. Moggi, Inorg. Chem. 7 (1968) 1398.
[61] H. Seki, K. Okada, Y. Iimura, M. Hoshino, J. Phys. Chem. A 101 (1997) 8174.
[62] M. Hoshino, Y. Nagashima, H. Seki, M. De Leo, P.C. Ford, Inorg. Chem. 37 (1998) 2464.
[63] A. Jr.Vlček, S. Záliš, Coord. Chem. Rev. 251 (2007) 258 and references herein.